



## Microfluidic cartridge with integrated array of amorphous silicon photosensors for chemiluminescence detection of viral DNA



M. Zangheri<sup>a</sup>, M. Mirasoli<sup>a,\*</sup>, A. Nascetti<sup>b</sup>, D. Caputo<sup>c</sup>, F. Bonvicini<sup>d</sup>, G. Gallinella<sup>d</sup>, G. de Cesare<sup>c</sup>, A. Roda<sup>a</sup>

<sup>a</sup> Department of Chemistry "Giacomo Ciamician", University of Bologna, Italy

<sup>b</sup> Aerospace Engineering School, Sapienza University of Rome, Italy

<sup>c</sup> Department of Information, Electronics and Communication Engineering, Sapienza University of Rome, Italy

<sup>d</sup> Department of Pharmacy and Biotechnology, University of Bologna, Italy

### ARTICLE INFO

#### Article history:

Received 2 November 2015

Received in revised form 9 January 2016

Accepted 11 January 2016

#### Keywords:

Integrated analytical system  
Amorphous silicon photosensors  
Chemiluminescence  
Nucleic acids detection  
Oligonucleotide array  
Point-of-care

### ABSTRACT

Portable and simple analytical devices based on microfluidics with chemiluminescence detection are particularly attractive for point-of-care applications, offering high detectability and specificity in a simple and miniaturized analytical format. Particularly relevant for infectious disease diagnosis is the ability to sensitively and specifically detect target nucleic acid sequences in biological fluids. To reach the goal of real-life applications for such devices, however, several technological challenges related to full device integration are still to be solved, one key aspect regarding on-chip integration of the chemiluminescence signal detection device. Nowadays, the most promising approach is on-chip integration of thin-film photosensors.

We recently proposed a portable cartridge with microwells aligned with an array of hydrogenated amorphous silicon (a-Si:H) photosensors, reaching attomole level limits of detection for different chemiluminescence model reactions. Herein, we explore its applicability and performance for multiplex and quantitative detection of viral DNA. In particular, the cartridge was modified to accommodate microfluidic channels and, upon immobilization of three oligonucleotide probes in different positions along each channel, each specific for a genotype of Parvovirus B19, viral nucleic acid sequences were captured and detected.

With this system, taking advantage of oligoprobes specificity, chemiluminescence detectability, and photosensor sensitivity, accurate quantification of target analytes down to  $70 \text{ pmol L}^{-1}$  was obtained for each B19 DNA genotype, with high specificity and multiplexing ability. Results confirm the good detection capabilities and assay applicability of the proposed system, prompting the development of innovative portable analytical devices with enhanced sensitivity and multiplexed capabilities.

© 2016 The Authors. Published by Elsevier B.V. This is an open access article under the CC BY-NC-ND license (<http://creativecommons.org/licenses/by-nc-nd/4.0/>).

### 1. Introduction

The need for portable and simple analytical devices that can be used at the point-of-care (POC) for real-time analysis of samples and timely accurate diagnosis is a major driving force for the development of integrated lab-on-chip devices that combine several laboratory functions on a single chip [1].

Particularly relevant for POC applications, such as infectious disease diagnosis, is the ability to sensitively and specifically detect target nucleic acid sequences in biological fluids.

Among optical detection strategies, chemiluminescence (CL) offers the advantages of high detectability in low volumes and simple instrumentation required for its measurement (no lamps, filters, or specific optical arrangements) [2]. Indeed, CL, i.e., the generation of photons by a chemical reaction, and particularly enzyme-catalyzed CL, has

been shown to provide superior analytical performance in miniaturized analytical formats [3,4].

Despite several applications described in the literature, one of the main challenges that needs to be faced for achieving commercial success is integration. Differently from colorimetric-based assays, in which visual observation or microspectrophotometers can be exploited, CL assays most often require a separate instrument to measure light emission, thus limiting its market exploitability and integration degree [5]. Smartphone CMOS cameras can be exploited as portable luminometers for on-site CL quantitative measurements, although ultrahigh detectability cannot be yet reached with such devices [6].

Recently, on-chip integration of organic [7] and inorganic [8] photosensors has been proposed to enable highly sensitive detection of CL reactions, thus prompting the development of innovative portable analytical devices with enhanced sensitivity and multiplexed capabilities.

In particular, starting from the pioneer paper of Kamei et al. [9], different research groups are focused on the development of

\* Corresponding author.

hydrogenated amorphous silicon (a-Si:H) photosensors to achieve on-chip detection within a lab-on-chip [10]. Taking advantage of the low-temperature deposition process (below 250 °C), a-Si:H photosensors can be grown on glass and polymers, ideal supports for lab-on-chip devices. This feature is coupled with two very important optoelectronic characteristics: a very low dark current in reverse bias, which determines a very low detection limit with respect for example to organic-based photosensors [3] and a quite high photosensitivity in the ultraviolet [11] and in the visible [12,13] range, which determine, even in the absence of a sensor cooling system, analytical performances in lab-on-chip application comparable to those achieved with cooled CCD imagers [14,15].

We have recently proposed an integrated cartridge in which an array of 16 a-Si:H photosensors was employed to independently monitor as many CL or bioluminescence reactions, showing its excellent analytical performance and reaching attomole level limits of detection [14]. Herein, we further explored the applicability and performance of such integrated device in diagnostics, i.e., detection and typization of Parvovirus B19 DNA, which was selected as a model analyte.

For this purpose, a disposable portable microfluidic cartridge with integrated a-Si:H photosensors has been developed and employed for multiplex detection of Parvovirus B19 genotypes exploiting oligonucleotide array capture and CL detection. The cartridge is composed of a glass slide on which an array of thin film a-Si:H photosensors has been deposited on one side, while the opposite side has been arrayed with three B19 genotype specific probes and coupled with polydimethylsiloxane (PDMS) microfluidic layer. Biotin-labeled targets were captured by genotype-specific immobilized probes and then hybrids were detected by means of an avidin-horseradish peroxidase (HRP) conjugate and CL reaction. To enable POC applicability, all the hybridization assay protocol does not require specific conditions regarding cleanliness, refrigeration or temperature control and fluid delivery is based only on capillary forces. Moreover the analysis could be performed employing a low amount of sample (50 µL), within less than 1 h. Portable custom electronics was employed for read-out of the CL signals that were detected by the a-Si:H photosensors, each placed in correspondence of one capture oligonucleotide spot. The results are easily readable and there is no need of specialized personnel for their interpretation, since the detection of the target analyte is simply ascribable to the presence of a photon emission.

## 2. Materials and methods

### 2.1. Chemicals

Silane-prep silanized microscope slides (26 × 76 mm<sup>2</sup>), HRP-labeled streptavidin, non-fat dried milk, glutaraldehyde and glycerol were purchased from Sigma-Aldrich (St. Louis, MO). The 25-mer biotin-labeled target sequences (Bio-5'-GGTCTGCCAAAGGTGTGTAAGAAGGC-3' for G1, Bio-5'-GGTCTGCCAGTGGAGTGAAAAGGC-3' for G2, and Bio-5'-GATC TGCCAGTGGCGTGTAAAAAGC-3' for G3) and the 25-mer amino-labeled oligonucleotide probes (NH<sub>2</sub>-C12-5'-GCCTTCTACACACCTTTG GCAGACC-3' for G1, NH<sub>2</sub>-C12-5'-GCCTTTTACTACTCCACTGGCAGACC-3' for G2, and NH<sub>2</sub>-C12-5'-GCTTTTACACGCCACTGGCAGATC-3' for G3) were purchased from Eurofins MWG Operon (Ebersberg, Germany). All other reagents were of analytical grade and were used as purchased.

The SuperSignal ELISA Femto CL substrate for HRP was obtained from Thermo Fisher Scientific, Inc. (Rockford, IL). The Silgard 184 PDMS prepolymer and the curing agent were obtained from Dow Corning (Midland, MI).

Phosphate buffered saline (PBS) was prepared as follows: 10 mmol L<sup>-1</sup> Na<sub>2</sub>HPO<sub>4</sub>, 2 mmol L<sup>-1</sup> KH<sub>2</sub>PO<sub>4</sub>, 137 mmol L<sup>-1</sup> NaCl, 2.7 mmol L<sup>-1</sup> KCl (pH 7.4). Borate buffered saline was prepared using 10 mmol L<sup>-1</sup> sodium borate and 150 mmol L<sup>-1</sup> NaCl (pH 9.5).

Hybridization buffer was composed by 0.3 mol L<sup>-1</sup> NaCl, 0.1 mol L<sup>-1</sup> TrisCl, 0.01 mol L<sup>-1</sup> EDTA, 0.1% Tween-20.

### 2.2. Photosensor array and electronic read-out board

The basic structure of a single photosensor of the array is a stack of Indium Tin Oxide (ITO)/a-SiC:H p-type/a-Si:H intrinsic/a-Si:H n-type/metal layers. In particular, the three a-Si:H layers have been deposited by Plasma Enhanced Chemical Vapor Deposition (PECVD) at 13.56 MHz in a three-chamber Ultra High Vacuum (UHV) deposition system. In each chamber the deposition of only one specific type of layer takes place. A load lock chamber, connecting the three UHV chamber, is dedicated to the sample loading and transfer between the three chambers. This procedure avoids dopant contamination between the chambers, resulting in a low defect density in the intrinsic material [16].

Table I reports the deposition parameters of the three a-Si:H layers. The deposition times and the gas mixtures have been optimized to achieve a low dark current and high responsivity in the visible range [17]. In particular, the presence on methane in the gas mixture deposition of the p-type layer leads to an increase of the energy gap of this region and to an increase of the photoresponse at short wavelengths.

The fabrication process of the complete array is based on the standard microelectronic techniques and is a four-mask process. Briefly, a 180 nm-thick ITO layer, which acts as transparent bottom contact of the diodes, has been deposited by magnetron sputtering on a 5 × 5 cm<sup>2</sup> ultrasonically cleaned glass substrate and patterned by Reactive Ion Etching (RIE). Subsequently, the p-i-n a-Si:H stacked structure with thickness equal to 10, 150 and 50 nm, respectively, has been deposited by PECVD followed by the deposition by vacuum evaporation of a three-metal Cr/Al/Cr 30/200/30 nm stack, which acts as top contact of the sensors. The area of the sensors, organized in an array of 5 × 6 matrix, has been then defined through wet etching of the Cr/Al/Cr stack and RIE of the a-Si:H layers. The mesa process has been followed by the deposition of a 5 µm-thick SU8-3005 (from Micro-Chem, MA, U.S.A.) and its patterning for opening via holes over the diodes. The holes are filled by a 150 nm-thick titanium/tungsten deposited through magnetron sputtering. The last photolithographic process refers to the wet etching of a 150 nm-thick titanium/tungsten alloy layer for the

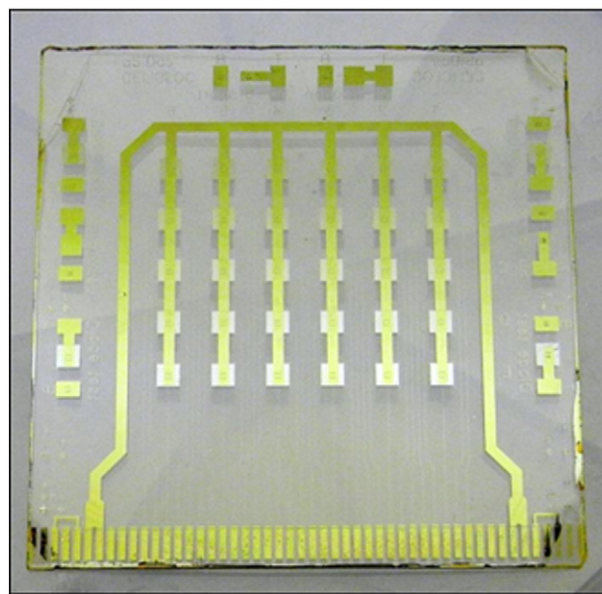


**Fig. 1.** Scheme of the array of a-Si:H photosensors: photosensors (30 light-gray squares) and top contact of the diodes (light-green U-shaped line). The array has dimensions 5 × 5 cm.

definition of the top grid electrodes and of the connection to the pad. A picture of the completed array is reported in Fig. 1.

The 30 light-gray squares, in the center of the picture, are the photosensors, while the light-green U-shaped line is the common top contact of the diodes. The front contact, connected to the p-layer of each diode, is not visible due to the transparency of the ITO layer.

The area of each diode is  $2 \times 2 \text{ mm}^2$ , while the pitch of the array is 5 mm. The area has been designed taking into account the dimension of the spot where the probes have been immobilized and the thickness of the glass substrate through which the CL signal propagates to reach the photodiodes deposited on the opposite face. The pitch of the array is a trade-off between the requirements of density of detection sites and low cross-talk between the photosensors [18]. It is also important to note that the use of a transparent substrate, as glass, reduces the distance between the photosensors and the site where the luminescence takes place [19] resulting in a reduced optical loss while ensuring a perfect separation between the 'chemical' side and the 'optoelectronic' side. This configuration therefore ensures a good reliability preventing faults that may generate from the interaction of sample and reagents with the electrical part of the cartridge.

Current–voltage characterization of all the photodiodes of the array, measured in dark conditions, show very low values of the dark current, which is around 10 pA when the diodes are reverse biased at 0.1 V. The parasitic parallel resistance is very high (above  $400 \cdot 10^9 \Omega$ ), thus ensuring a low dependence of the dark current with the sensor bias. Taking into account that the band B of the measurements is about 1 Hz, the shot noise current contribution does not overcome 10 fA. The spectral response of the device has been characterized through quantum efficiency measurement between 400 nm and 800 nm. In particular, at 425 nm, that is the wavelength at which the peak of the CL emission spectrum occurs, the QY is equal to 0.36 with a corresponding responsivity of 130 mA/W.

The electronic board, dedicated to the readout of the current photosensors, combines measurement of currents ranging from femtoamps to microamps, on-board bias-voltage supply, USB and UART interface, USB or external unregulated power supply operation, low power consumption and compact board size ( $70 \times 70 \text{ mm}^2$ ) [20]. The core of the electronic board are the DDC118 Current-Input Analog-to-Digital Converter from Texas Instruments used as low-noise sensor front-end and the microcontroller PIC18F4550 from Microchip that provides the timing and control as well as the communication interfaces, both USB and UART, to a PC. A software, developed in Java, allows to set all the measurement parameters.

The characterization of the noise performance of the electronic board has been performed connecting the photodiodes to the board and biasing them at low reverse voltage (25 mV). By using a 50 pF integration capacitance and a 200 ms integration time, we found that the total measurement noise, sum of the dark current noise and the electronic noise, is less than 40 fA.

The combination of this very good noise performance and of the good sensor photosensitivity allows achieving analytical performance that can be successfully applied to different assays as will be shown below.

### 2.3. Analytical device

The analytical device employed a disposable reaction cartridge consisting of a silanized microscope glass slide with an array of immobilized probes spots coupled with a PDMS fluidic element. To immobilize the probes, the silanized glass slide was previously activated according to a literature protocol [21] by soaking for 2 h at room temperature in a 2.5% (v/v) solution of glutaraldehyde in PBS. The slide was rinsed with ethanol and distilled water, then air-dried. The amino-labeled genotype specific oligoprobes diluted in borate buffer, containing 0.1% (v/v) glycerol were then spotted (0.2 pmol/spot) in triplicate in an array of nine ( $3 \times 3$ ) spots, each one not exceeding 1 mm in

diameter and 3 mm spacing. The slide was incubated for 1 h at room temperature in a humid chamber to allow coupling between the primary amino groups of probes and the aldehyde groups of the functionalized glass surface. It was then washed with PBS ( $3 \times 5 \text{ min}$ ) and the remaining free reactive sites were saturated by soaking the slide in a blocking solution (PBS containing 5% (w/v) non-fat dried milk) for 2 h at room temperature. After a further washing with PBS (5 min) followed by air-drying, the slide was ready to be coupled with the PDMS elements, taking care that the probe spots were in the correspondence of the channels of the PDMS element (Fig. 2b). The fluidic element was prepared by mixing PDMS prepolymers with the curing agent in a 10:1 (w/w) ratio. The mixture was degassed under vacuum for 30 min, then poured in the casting master and incubated overnight at 25 °C to allow PDMS polymerization [22]. According to the design of the casting master, parallel channels (32.0 mm length, 2.0 mm width, 0.05 mm height) were engraved in the final fluidic element, each of them connected to a 50- $\mu\text{L}$  inlet reservoir for loading samples and reagents (Fig. 2a). The partial sticky nature of not-fully cured PDMS was exploited to obtain sufficient adhesion with the glass surface.

### 2.4. Assay protocol

For calibration curves, 50  $\mu\text{L}$  of hybridization buffer containing the artificial targets at different concentrations (from 0.08 to 100  $\text{nmol L}^{-1}$ ), were dispensed in the inlet reservoir and let flowing through the channels. Upon washing step performed with 100  $\mu\text{L}$  of PBS to remove nonspecific DNA–DNA hybrids, 50  $\mu\text{L}$  of HRP-labeled avidin (50  $\mu\text{g L}^{-1}$  in hybridization buffer) was added in each channel. Then a further washing was performed with 100  $\mu\text{L}$  of PBS. Finally 20  $\mu\text{L}$  of SuperSignal ELISA Femto was dispensed in the inlet reservoir, the reaction chip was positioned directly on the glass support where the 30-photosensor array had been deposited. Each spotted probe is aligned with a photosensor that is used to monitor the correspondent CL signal. After enclosing the system in a dark box and connecting photosensors to a personal computer, it is possible to acquire CL signal (Fig. 2c). Therefore, the complete protocol is performed inside the small dark box which contains: (1) the electronic board dedicated to the readout of the photosensors current; (2) a board that constitutes an interface between the previous one and the photosensors array; (3) the photosensors array; (4) the microfluidic chip. The time required to perform the entire analysis was 20 min since each step required about 5 min depending on the dispensed volume. The luminescent signal was monitored with the a-Si:H photosensors through consecutive 200-ms acquisitions.

### 2.5. Signal detection and elaboration

The measurement of the luminescence signals were performed with a delay of 20 s after the closure of the dark box to ensure that the signal measured by the photosensors was not altered by a memory effect due to exposure to ambient light [23]. Each point in the calibration curve corresponds to plateau value of photocurrent measured during the steady state emission. The mean photon emission measured from each probe spot was corrected by subtracting the signal measured by neighboring photosensors. The analytical performances of the photosensors were compared with that of a conventional ultrasensitive imaging instrument, ATIK 11002 Monochromatic (Norwich, UK), employing a previously described CCD-based contact imaging configuration [24]. In particular the glass slide was placed directly in contact with the thermoelectrically-cooled CCD sensor through a round fiber optic taper. This assembly was shielded from ambient light enclosing it in a proper case. During the acquisition the CCD sensor temperature was kept at 4 °C. Using ImageJ software v. 1.46 (National Institute of Health, Bethesda, MD) for the elaboration of the signal, the mean photon emission intensity was measured in the areas corresponding to

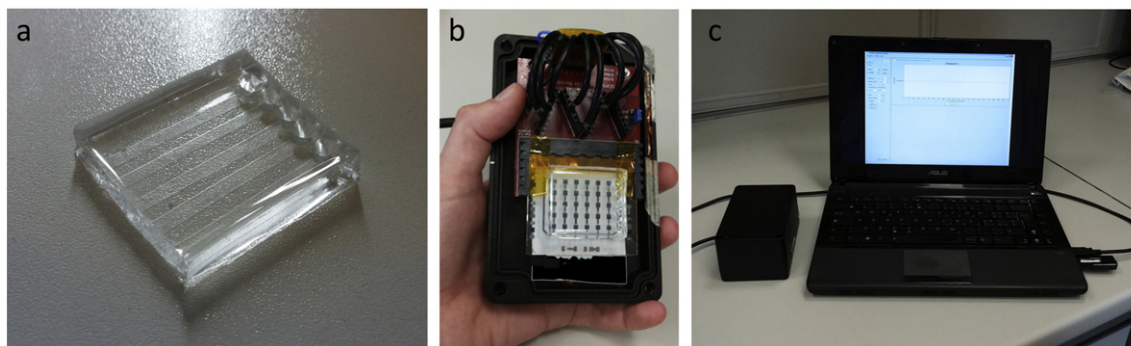


**Fig. 2.** a) PDMS fluidic element; b) analytical device assembled with photosensors array; c) detection performed enclosing the photosensors in a dark box and acquiring data through a personal computer.

probe spots. Each was subtracted from the mean background signal measured in adjacent areas and expressed in relative light units.

The reported limits of detection (LOD) both for photosensors and CCD, were calculated as the concentration whose signal corresponds to three times the standard deviation of the blank signal, which is the signal measured in the absence of the target analyte. Such standard deviation accounts for electronic noise, instrumental noise, as well as the variation of the low autoluminescence of the CL cocktail.

### 3. Results

Microfluidic analytical devices with optical detection are considered one of the best options for developing robust and sensitive lab-on-chip devices. Key features for diagnostic and prognostic usefulness of such devices are high sensitivity and specificity, ability to provide quantitative information and multiplexing capability. On the other hand, one of the main challenges for real life applications and commercial exploitation is full integration, which includes the open issue of coupling the lab-on-chip with a portable and miniaturized detector [1].

The use of CL detection in a disposable microfluidic chip with integrated array of a-Si:H photosensors has been previously shown to provide excellent analytical performance in enzyme assays and immunoassays applications, along with detector on-chip integration, optimal optical coupling, device compactness and reduced power consumption and memory occupancy [14].

As of today, the gold standard for the detection of a target pathogen for diagnostic purposes is to identify and possibly quantify its specific nucleic acid sequences. We therefore explored the suitability of the device for multiplex quantitative detection of nucleic acid sequences relevant for infectious disease diagnosis application.

#### 3.1. Calibration curves for the three B19 genotypes and comparison with CCD detection

The calibration curves, generated for each B19 genotype employing complementary biotin-labeled artificial targets in concentration range from  $0.08 \text{ nmol L}^{-1}$  to  $100 \text{ nmol L}^{-1}$ , are reported in Fig. 3a.

The LOD value was  $0.07 \text{ nmol L}^{-1}$  for all the B19 target, corresponding to  $4.3 \times 10^7 \text{ molecules L}^{-1}$ , and the dynamic range of the assay extended to  $100 \text{ nmol L}^{-1}$ , covering four orders of magnitude of target concentration.

When the same format was tested using a CCD camera as detector a LOD value of  $0.08 \text{ nmol L}^{-1}$  was obtained for all the B19 targets (Fig. 3b), confirming the result obtained in a previous work in which a different model of CCD sensor was employed [25]. The obtained results are very promising considering that the CCD sensor was thermoelectrically cooled down to  $4 \text{ }^\circ\text{C}$ , which decreases the background signal (both in terms of absolute value and instrumental noise) due to the thermal generation of electrons, while the a-Si:H photosensors were employed at room temperature (about  $25 \text{ }^\circ\text{C}$ ) in view of their use in a POC setting as well as to avoid cooling down of biological reactions that occur on the opposite side of the same glass substrate, which would largely affect their kinetics. Moreover comparison with the LOD of  $0.1 \text{ nmol L}^{-1}$  obtained employing a conventional PCR-ELISA format, as shown in the previous work [25], demonstrates comparable performances with state-of-the-art laboratory instrumentation.

#### 3.2. Assay specificity

The genotype specific B19 capture probes were selected in a previous work to provide sensitive and selective detection of the different

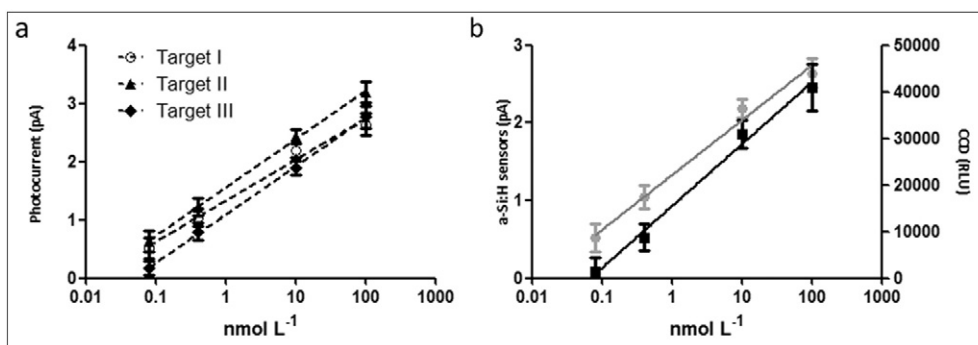


**Fig. 3.** a) Calibration curves obtained by DNA–DNA hybridization reactions between fully complementary B19 capture probe and artificial oligonucleotide targets for the three different genotypes; b) comparison of calibration curve obtained with a-Si:H photosensors (gray symbols) and with CCD camera (black symbols).

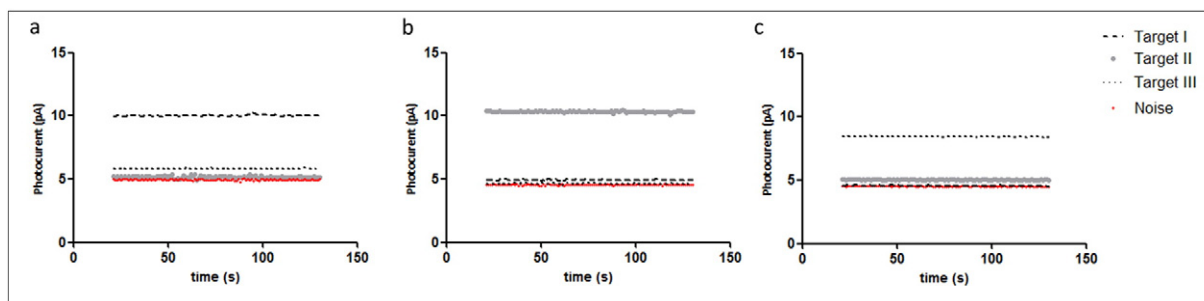


**Fig. 4.** Chemiluminescent signals obtained from hybridization reactions between the three amino-linked B19 DNA probes and the three biotin-labeled artificial oligonucleotides. The graphs show the CL response signals of three reaction chips, each one arrayed with three B19 genotype-specific probes (three separate spots per genotype) and hybridized with a defined B19 biotin-labeled target ((a) genotype 1, (b) genotype 2, (c) genotype 3).

B19 genotypes in microfluidic formats [25]. The assay specificity assessed in the previous work was evaluated also by using the array of photosensors for the analysis of different genotypes of B19 target ( $50 \text{ nmol L}^{-1}$ ). As shown in Fig. 4, CL signals above the LOD were observed only when the target analyte hybridized with the corresponding capture probe, confirming the results previously obtained. In addition, no significant CL signal was detected when the biotin-labeled B19 negative control target was assayed with each capture probe.

### 3.3. Signal detection

The array of photosensors allows to develop a system suitable for multiplex bioassays since it can provide the simultaneous measurements of 30 luminescent reactions. In this context it is important to ensure that all the photosensors respond equally to light signals and to verify the absence of crosstalk phenomena among adjacent photosensors. Since the genotype specific oligoprobes were spotted in triplicate, the inter-sensor reproducibility was assessed for each point of the calibration curve, finding a maximum variability of 12%. This variability can be ascribed to differences in the photoresponse of the sensors as well as to differences in the amount of solution spotted in each site. In order to distinguish the weight of each contribution, we assessed the variability of the CCD camera response for the same sites finding a maximum variability of 8%. Therefore variability ascribed to different responses of the photosensors is only 4%. Regarding the inter-site crosstalk phenomenon, it results negligible. In fact, injecting in the central channel the maximum target concentration, it was found that the signals detected by photosensors for the adjacent empty channels were comparable with the usual noise level of the sensors. In this way it was proved that the geometrical design of the array in terms of sensor size and spacing combined with design of the PDMS channels is suitable for the simultaneous measurement of the three B19 genotypes.

## 4. Conclusion

In the present work, the performance of a portable analytical device based on a disposable microfluidic cartridge integrated with an array of 30 a-Si:H photosensors for CL detection of viral DNA was evaluated. In particular a microfluidic reaction chip was designed comprising a PDMS microfluidic layer coupled with a glass slide on which genotype specific B19 capture oligonucleotide probes had been arrayed. The reaction chip was then integrated with the array of photosensors, aligning each photosensor with one oligonucleotide probe spot in order to monitor luminescent signals. Both the reaction chip and the a-Si:H photosensors are inexpensive to manufacture and suitable for the development of portable analytical devices. The design of the reaction chip combined with the array of photosensors make it possible to detect simultaneously three B19 DNA in a unique analysis. Moreover the specificity of the oligoprobes and the sensitivity of photosensors allowed an

accurate quantification of the target analyte. In fact, target detectability was  $0.07 \text{ nmol L}^{-1}$  for the three different B19 DNA genotypes which is comparable to the LOD of  $0.1 \text{ nmol L}^{-1}$  obtained both for the DNA hybridization step of B19 amplified products in conventional assay formats (e.g., PCR-ELISA methods) or exploiting other portable detection systems (e.g., CCD camera) [25]. Moreover the photosensors showed low instrumental noise levels, good reproducibility and negligible crosstalk between adjacent sensors.

This minimally instrumented system can be implemented with the integration of a miniaturized PCR system in order to obtain the full POC applicability. Furthermore, thanks to the simple configuration and the ease-of-use, the proposed device could be adapted for different analytes, simply by changing the arrayed probes.

It is finally worth considering that the presented system has all the features and potentialities to be a low cost system, since the read-out electronic system and the a-Si:H photosensor array are based on well-mature technologies, whose cost is dependent only on the number of produced pieces, and the microfluidic chip relies on PDMS technology, that can be easily developed and produced.

## Acknowledgments

Financial support was provided by the Italian Ministry of Instruction, University and Research (MIUR): PRIN 2010-2011 project: prot. 20108ZSRTR “ARTEMIDE (Autonomous Real Time Embedded Multi-analyte Integrated Detection Environment): a fully integrated lab-on-chip for early diagnosis of viral infections”.

## References

- [1] N.M.M. Pires, T. Dong, U. Hanke, N. Hoivik, Recent developments in optical detection technologies in lab-on-a-chip devices for biosensing applications, *Sensors* 14 (2014) 15458–15479.
- [2] M. Mirasoli, M. Guardigli, E. Michelini, A. Roda, Recent advancements in chemical luminescence-based lab-on-chip and microfluidic platforms for bioanalysis, *J. Pharm. Biomed. Anal.* 87 (2014) 36–52.
- [3] A. Roda, M. Guardigli, E. Michelini, M. Mirasoli, P. Pasini, Analytical bioluminescence and chemiluminescence, *Anal. Chem.* 75 (2003) 462A–470A.
- [4] M. Seidel, R. Niessner, Chemiluminescence microarrays in analytical chemistry: a critical review, *Anal. Bioanal. Chem.* 406 (2014) 5589–5612.
- [5] J.Y. Park, L.J. Kricka, Prospects for the commercialization of chemiluminescence-based point-of-care and on-site testing devices, *Anal. Bioanal. Chem.* 406 (2014) 5631–5637.
- [6] A. Roda, M. Guardigli, D. Calabria, M.M. Calabretta, L. Cevenini, E. Michelini, A 3D-printed device for a smartphone-based chemiluminescence biosensor for lactate in oral fluid and sweat, *Analyst* 139 (2014) 6494–6501.
- [7] X. Wang, M. Amatongchai, D. Nacapricha, O. Hofmann, J.C.d. Mello, D.D.C. Bradley, A.J.d. Mello, Thin-film organic photodiodes for integrated on-chip chemiluminescence detection—application to anti-oxidant capacity screening, *Sensors Actuators B Chem.* 140 (2009) 643–648.
- [8] P. Novo, D.M. Prazeres, V. Chu, J.P. Conde, Microspot-based ELISA in microfluidics: chemiluminescence and colorimetry detection using integrated thin-film hydrogenated amorphous silicon photodiodes, *Lab Chip* 11 (2011) 4063–4071.
- [9] T. Kamei, B.M. Paegel, J.R. Scherer, A.M. Skelley, R.A. Street, R.A. Mathies, Integrated hydrogenated amorphous Si photodiode detector for microfluidic bioanalytical devices, *Anal. Chem.* 75 (2003) 5300–5305.

- [10] D. Caputo, M. Ceccarelli, G. de Cesare, A. Nascetti, R. Scipinotti, Lab-on-glass system for DNA analysis using thin and thick film technologies, *P. Mat. Res. Sym.*, 1191, 2009 (0006-01).
- [11] A.C. Pimentel, A.T. Pereira, V. Chu, D.M.F. Prazeres, J.P. Conde, Detection of chemiluminescence using an amorphous silicon photodiode, *IEEE Sensors J.* 7 (2007) 415–416.
- [12] D. Caputo, G. de Cesare, C. Fanelli, A. Nascetti, A. Ricelli, R. Scipinotti, Amorphous silicon photosensors for detection of Ochratoxin A in wine, *IEEE Sensors J.* 12 (2012) 2674–2679.
- [13] R. Martins, P. Baptista, L. Raniero, G. Doria, L. Silva, R. Franco, E. Fortunato, Amorphous/nanocrystalline silicon biosensor for the specific identification of unamplified nucleic acid sequences using gold nanoparticle probes, *Appl. Phys. Lett.* 90 (2007) 023903.
- [14] M. Mirasoli, A. Nascetti, D. Caputo, M. Zangheri, R. Scipinotti, L. Cevenini, G. de Cesare, A. Roda, Multiwell cartridge with integrated array of amorphous silicon photosensors for chemiluminescence detection: development, characterization and comparison with cooled-CCD luminograph, *Anal. Bioanal. Chem.* 406 (2014) 5645–5656.
- [15] D. Caputo, G. de Cesare, L.S. Dolci, M. Mirasoli, A. Nascetti, A. Roda, R. Scipinotti, Microfluidic chip with integrated a-Si:H photodiodes for chemiluminescence-based bioassays, *IEEE Sensors J.* 13 (2013) 2595–2602.
- [16] D. Caputo, G. de Cesare, F. Irrera, F. Palma, M. Tucci, Characterization of intrinsic a-Si:H in p-i-n devices by capacitance measurement: theory and experiment, *J. Appl. Phys.* 76 (6) (1994) 3534–3541.
- [17] D. Caputo, G. de Cesare, A. Nascetti, R. Scipinotti, Amorphous silicon photosensors for on-chip detection in digital microfluidic system, *Sensor. Actuat. A- Phys.* 216 (2014) 1–6.
- [18] D. Caputo, A. de Angelis, N. Lovecchio, A. Nascetti, R. Scipinotti, G. de Cesare, Amorphous silicon photosensors integrated in microfluidic structures as a technological demonstrator of a “true” lab-on-chip system, *Sens. Bio-Sens. Res.* 3 (2015) 98–104.
- [19] C.R. Vistas, S.S. Soares, R.M.M. Rodrigues, V. Chu, J.P. Conde, G.N.M. Ferreira, An amorphous silicon photodiode microfluidic chip to detect nanomolar quantities of HIV-1 virion infectivity factor, *Analyst* 139 (2014) 3709–3713.
- [20] A. Nascetti, G. Colonia, D. Caputo, M. Tavernelli, P. Placidi, A. Scorzoni, G. de Cesare, Multi-channel very-low-noise current acquisition system with on-board voltage supply for sensor biasing and readout, *Procedia Eng.* 87 (2014) 1577–1580.
- [21] G.T. Hermanson, *Bioconjugate Techniques*, second ed. Academic Press, San Diego, 2008.
- [22] H. Cong, T. Pan, Photopatternable conductive PDMS materials for microfabrication, *Adv. Funct. Mater.* 18 (2008) 1912–1921.
- [23] H. Wiczorek, Effect of trapping in a-Si H diodes, *Solid State Phenom.* 44 (1995) 957–972.
- [24] A. Roda, M. Mirasoli, L.S. Dolci, A. Buragina, F. Bonvicini, P. Simoni, M. Guardigli, Portable device based on chemiluminescence lensless imaging for personalized diagnostics through multiplex bioanalysis, *Anal. Chem.* 83 (2011) 3178–3185.
- [25] M. Mirasoli, F. Bonvicini, L.S. Dolci, M. Zangheri, G. Gallinella, A. Roda, Portable chemiluminescence multiplex biosensor for quantitative detection of three B19 DNA genotypes, *Anal. Bioanal. Chem.* 405 (2013) 1139–1143.